applied sciences

MDPI

Article

Numerical and Experimental Ground Vibration Test of Composite Flying Wing

Maciej Milewski [1,*], Jakub Wróbel [1], Mateusz Kucharski [1], Krzysztof Kaliszuk [1], Bartłomiej Dziewoński [1], Jacek Napora [2], Tomasz Kisiel [1], Paweł Bury [1] and Artur Kierzkowski [1,*]

[1] Department of Technical System Operation and Maintenance, Faculty of Mechanical Engineering, Wroclaw University of Science and Technology, Smoluchowskiego 48, 50-372 Wroclaw, Poland; jakub.wrobel@pwr.edu.pl (J.W.); m.kucharski@pwr.edu.pl (M.K.); krzysztof.kaliszuk@pwr.edu.pl (K.K.); bartlomiej.dziewonski@pwr.edu.pl (B.D.); tomasz.kisiel@pwr.edu.pl (T.K.); pawel.bury@pwr.edu.pl (P.B.)

[2] Faculty of Mechanical and Power Engineering, Wroclaw University of Science and Technology, Stanisława Wyspiańskiego 27, 50-372 Wroclaw, Poland; 247066@student.pwr.edu.pl

* Correspondence: maciej.milewski@pwr.edu.pl (M.M.); artur.kierzkowski@pwr.edu.pl (A.K.)

Abstract

Ground vibration testing (GVT) plays a key role in the validation of numerical models and the assessment of aeroelastic stability in lightweight aircraft structures. This study presents an experimental and numerical investigation of a full-scale composite flying wing unmanned aerial vehicle (UAV) intended for vertical take-off and landing operations. Due to its low structural mass and highly integrated configuration, the aircraft exhibits increased sensitivity to modeling assumptions, boundary conditions, and measurement uncertainties. A finite element model was developed in Ansys, incorporating detailed laminate definitions and the internal sandwich structure. Experimental modal testing was performed under free-free boundary conditions using an electrodynamic shaker and a distributed measurement consisting of 94 response locations. Frequency Response Functions (FRFs), coherence analysis, and the Complex Mode Indication Function (CMIF) were employed to identify the dominant structural modes. Particular attention was given to the bending and torsional modes that govern aeroelastic behavior. Comparison of experimental and numerical results showed good agreement in mode shapes, while discrepancies in natural frequencies ranged from 10.4% to 20.1%. The results demonstrate that the model adequately captures the dynamic behavior of the aircraft and provides a reliable basis for future aeroelastic and flutter analyses of lightweight composite flying wing.

Keywords: ground vibration test; flying wing; UAV; composite structure

Academic Editor: Andrea Carpinteri

Received: 5 June 2026
Revised: 23 June 2026
Accepted: 24 June 2026
Published: 1 July 2026

1. Introduction

The rapid proliferation of unmanned aerial vehicles (UAVs) has led to their increasing operation in close proximity to populated areas. Applications such as urban monitoring, infrastructure inspection, and last-mile delivery require UAV platforms to operate directly over people, where structural reliability becomes a critical safety concern [1–6]. At the same time, market pressure enforces shortened development cycles, limiting the extent of experimental validation typically performed during the design process.

Lightweight structural design has become a fundamental requirement for modern UAV systems, driven by the need to maximize flight endurance, payload capacity, and overall operational efficiency [7–9]. For this reason, composite materials are widely adopted,

offering high stiffness-to-weight ratios and enabling the development of slender and aerodynamically efficient configurations [10]. However, the use of composites introduces additional challenges related to structural integrity and safety. Unlike isotropic materials, their behavior is strongly dependent on fiber orientation, layup configuration, and internal structural design [11,12]. In ultra-lightweight configurations, even minor modeling inaccuracies or experimental uncertainties may lead to substantial errors [13], making precise assessment of dynamic properties essential for safe operation.

Ground vibration testing (GVT) is foundational for ensuring the aeroelastic stability, structural integrity, and certification of modern aircraft, particularly those employing innovative flying wing configurations and advanced composite materials. The unique structural and aerodynamic characteristics of flying wings demand precise characterization of their dynamic behavior to prevent catastrophic failures such as flutter and to optimize performance [14]. In lightweight UAV structures, achieving reliable modal identification is particularly challenging due to low natural frequencies, high sensitivity to boundary conditions, and environmental disturbances. In composite aircraft structures, additional uncertainty arises from manufacturing variability, including deviations in fiber orientation, material property dispersion, and bonding quality in sandwich structures. These factors can significantly affect stiffness distribution and, consequently, the dynamic response of the structure. From an aeroelastic perspective, accurate identification of structural dynamic properties is essential for flutter prediction, which arises from the interaction between bending and torsional modes. The relative proximity of these modes in frequency domain, as well as their correct spatial representation, directly influences the stability boundaries of the system.

GVT is typically undertaken on entire aircraft—such as fighter jets, civil airliners, and unmanned aerial vehicles or on specific components like helicopter blades [15]. The main goal of these tests in aerospace is the extraction of modal parameters, which are used to update finite element models (FEM). Normally, the FEM is coupled with an aerodynamic model to predict aeroelastic behavior [16]. To achieve accurate correlation between the FEM and the physical structure, the FEM must be carefully tuned using GVT results, ensuring that the final design reflects the correct dynamic response and aeroelastic properties [17,18]. In the context of ultralight composite UAVs, where minor modeling errors or measurement uncertainties can have a significant impact, this tuning is critical both for safety and for reducing costly experimental testing. Similar approaches can be found in fluid-coupled structures, such as underwater glider wings, where the experimentally or numerically identified structural modal characteristics constitute the basis for subsequent hydroelastic analyses, resonance assessment, and vibration mitigation strategies [19]. While experimental modal analysis has been widely applied in conventional aeronautical structures, studies focusing on the validation of numerical models using experimental data for lightweight composite UAV configurations remain limited. Existing research has primarily addressed individual components, such as wings [20–22], often under simplified assumptions regarding boundary conditions and structural behavior. Although some work on blended wing–body UAVs [23] provides initial insight, the overall representation of ultralight, fully integrated configurations in modal analysis literature is still insufficient. Chakravarty [24] performed an experimental and numerical modal analysis of a flexible composite micro air vehicle (MAV) wing, combining non-contact measurement of membrane prestrain using visual image correlation with finite element simulations. Pavan Kishore et al. [25] conducted a finite element-based free vibration analysis of a composite aircraft wing, investigating the influence of design parameters such as fiber orientation, stacking sequence, and ply thickness on the natural frequencies and mode shapes. Tandel et al. [26] investigated the fluid–structure interaction and aeroelastic behavior of a high-aspect-ratio GFRP composite

wing through a combined numerical and experimental approach, integrating modal and aeroelastic analyses.

This gap is particularly significant in the case of flying wing structures, where the airframe acts as a single, load-carrying system rather than a set of distinguishable components. Such configurations introduce additional challenges in both experimental testing and numerical modeling, including the definition of appropriate boundary conditions, the implementation of representative excitation methods, and the accurate representation of composite sandwich structures with strong material anisotropy. These issues are further exacerbated by the low structural mass, where even small disturbances or modeling inaccuracies can significantly affect the identified dynamic response. Within this context, Ji et al. [27] developed a high-fidelity CFD/CSD/6DOF coupling framework for body freedom flutter prediction of a flying-wing aircraft, where the structural dynamic characteristics were obtained from a finite element modal analysis and subsequently used in aeroelastic simulations without experimental modal validation. Guo et al. [28] performed a finite element-based modal analysis of a composite flying-wing configuration as part of an aeroelastic investigation of a passive gust alleviation device, without experimental validation of the structural dynamic model. These studies highlight that, despite increasing complexity of aeroelastic simulations, experimental validation of modal behavior for integrated flying wing configurations remains limited.

Addressing these challenges is essential for improving the reliability of numerical simulations and ensuring safe operation under dynamic and aeroelastic loading conditions.

The aim of this study is to perform GVT of a fully composite flying wing and to develop a corresponding finite element model capable of accurately reproducing its dynamic behavior. Particular attention is given to the challenges associated with ultralight integrated structures, including suspension conditions, excitation strategy, and detailed representation of composite materials. The validated numerical model is intended to support reliable dynamic analysis while reducing the reliance on extensive experimental testing.

2. Materials and Methods

2.1. Test Object Description

The test object is a tailsitter flying wing UAV designed for vertical take-off and landing (VTOL) operations (Figure 1a). The aircraft is intended for rapid deployment missions, specifically for the delivery of automated external defibrillators (AEDs) in emergency scenarios. The structure has a wingspan of 1.9 m and a total structural mass of about 3 kg. Such a low mass relative to its size results in a highly flexible structure, making it particularly sensitive to dynamic effects and external disturbances.

The aircraft is constructed as a semishell composite structure. The composite shell is primarily responsible for carrying torsional loads, with fiber orientations in the wing sections arranged predominantly at $\pm 45^{\circ}$, enhancing torsional stiffness. A detailed description of the laminate configuration and material properties is provided in Table 1. The internal structure (Figure 1b) consists of spars and ribs manufactured from lightweight core materials (Herex), and is primarily responsible for carrying bending loads. The spars and ribs have a thickness of 5 mm. This internal framework provides the necessary stiffness while maintaining minimal mass.

Additionally, an internal aluminum cage with a thickness of 4 mm is integrated into the structure to accommodate and secure the AED payload.

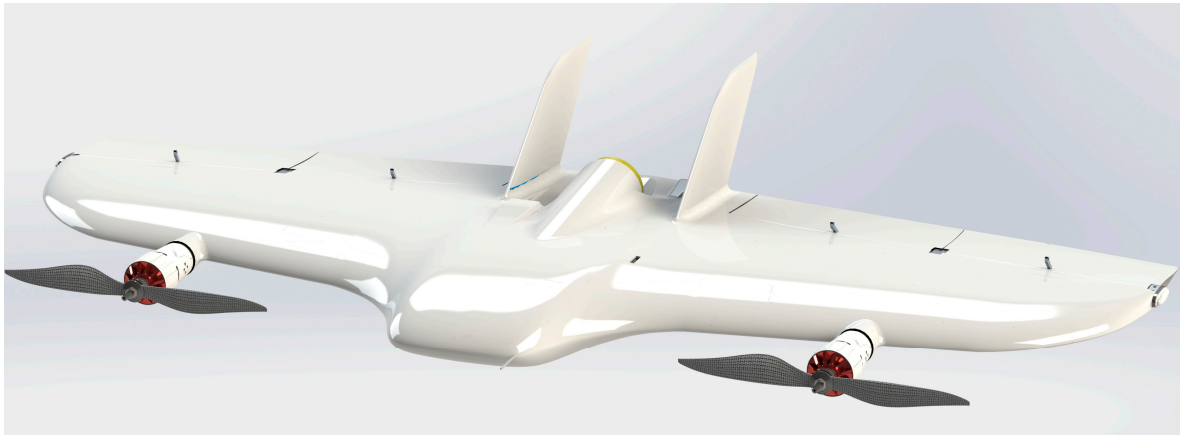

(**a**)

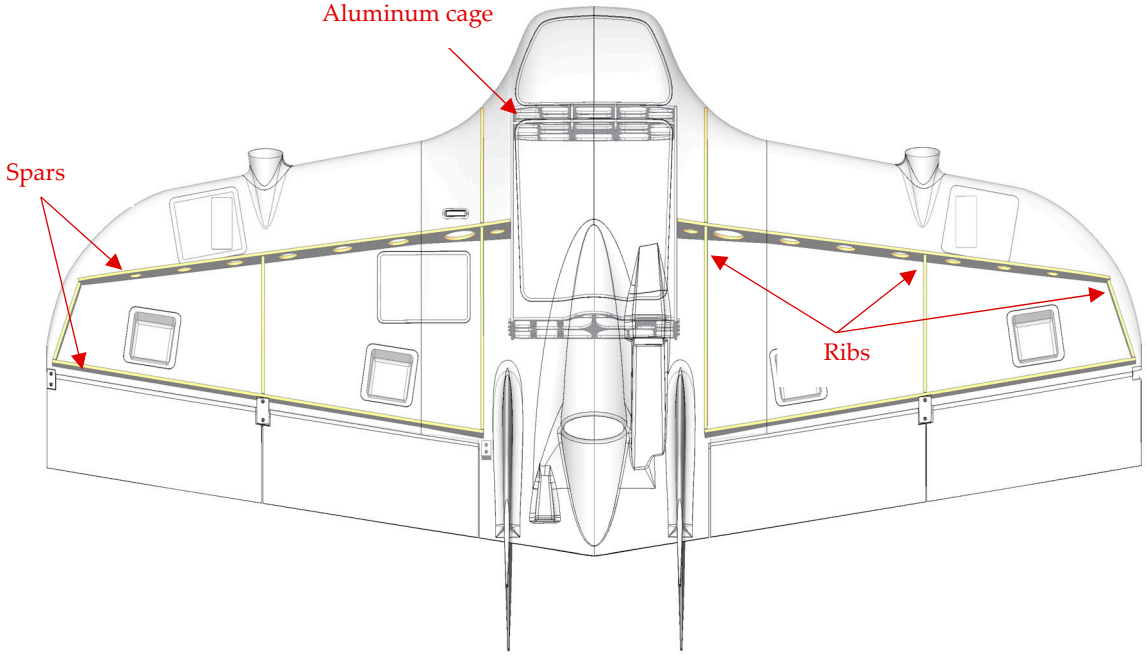

(**b**)

Figure 1. Test object. (**a**) isometric view of the aircraft. (**b**) internal structure of the aircraft.

Table 1. Lay-up configuration on the plane.

Ply (From Mold Side to Inner Surface)	Wing Section	Fuselage Section
1	CFRP CBX90 [±45°]	CFRP Torayca [0°/90°]
2	CFRP CBX90 [±45°]	CFRP Torayca [0°/90°]
3	Sandwich material	Sandwich material
4	CFRP CBX90 [±45°]	CFRP Torayca [0°/90°]
5	GFRP Interglass [0°/90°]	

2.2. Finite Element Model

The FEM was employed to investigate the dynamic behavior of the analyzed composite flying wing structure. The reliability of such simulations strongly depends on the appropriate definition of material parameters, geometric fidelity, and model calibration. It is well recognized that numerical models tend to overestimate structural stiffness; therefore, experimental validation is essential to ensure accurate representation of the physical system [29,30].

Numerical simulations were performed using the ANSYS 2024 R2 Workbench environment, with particular emphasis on the Ansys Composite Prep/Post (ACP) module. This tool enables detailed modeling of laminated composite structures, allowing precise definition of material properties, layer thickness, and fiber orientation for each ply. The ability to reproduce complex layup sequences is critical, as fiber orientation significantly influences the global stiffness and dynamic response of the structure. In the present study, a fully composite sandwich configuration was modeled, accounting for both skin laminates and internal structural components.

The modeling process began with the development of a CAD model representing the flying wing geometry. Due to the high geometric complexity of the structure, simplifications were introduced to ensure numerical tractability and solver stability. Non-essential geometric details were removed while preserving the overall stiffness distribution and load paths. The simplified geometry was then imported into the simulation environment, where further preprocessing steps were conducted.

The wing structure was modeled using a combination of shell and solid elements. The composite skins were represented using shell elements (SHELL181), divided into upper and lower surfaces to reflect the actual manufacturing process and enable accurate assignment of laminate stacking sequences. The internal structure, including ribs and spars, was discretized using solid elements (SOLID186). A mesh size of 8 mm was applied to the shell model, while a finer mesh size of 2 mm was used for internal structural components to ensure adequate resolution of stiffness variations. The mesh on the structure is shown in Figure 2. The final model consisted of 242,309 elements, with an average mesh quality of 0.92.

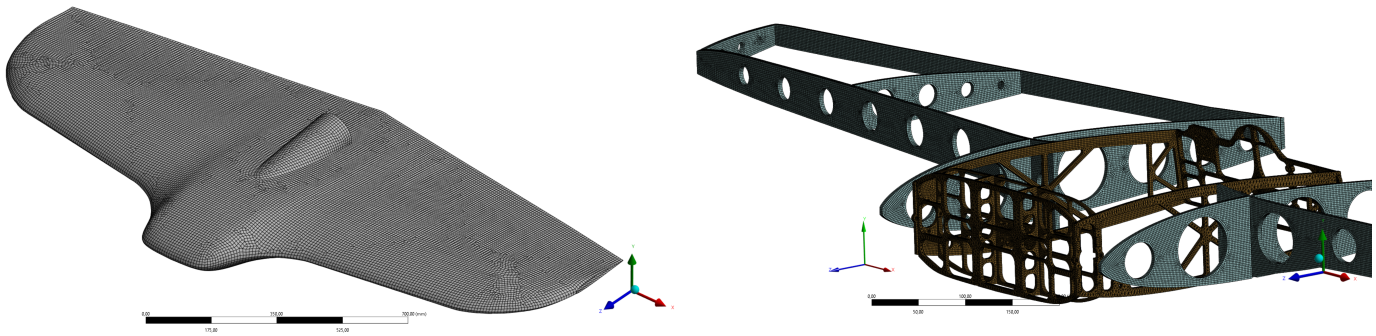

(**a**) (**b**)

Figure 2. Mesh on the structure of drone. (**a**) Shell structure consisting of 37,268 elements. (**b**) The internal structure consisting of 205,041 elements.

The orthotropic behavior of each layer was considered through the definition of fiber orientations and stacking sequences. This approach allows for capturing the anisotropic stiffness characteristics that are critical for accurate dynamic analysis. The layup with direction of plies is shown in Figure 3.

To ensure realistic interaction between structural components, contact definitions were introduced between the shell model and internal structural elements, as well as between individual structural parts. Since the components are physically bonded in the manufacturing process, a bonded contact formulation was employed. Specifically, the bonded contact was implemented using the Multi-Point Constraint (MPC) algorithm with the Nodal-Projected Normal From Contact detection method and Dual Shape Function formulation. This approach enforces displacement compatibility across the contact interface and transfers loads without allowing relative motion or separation between the connected surfaces. The material properties assigned in the numerical model were determined based on an experimental material characterization conducted in accordance with ASTM D3039,

ASTM D6641, and ASTM D7078 standards [31–33]. These tests provided the mechanical properties required for the orthotropic material definition of the composite laminates used in the finite element model. The resulting material parameters are summarized in Table 2. Herex properties were assigned based on Ansys library. A Herex thickness of 1.2 mm was assigned according to manufacturing value.

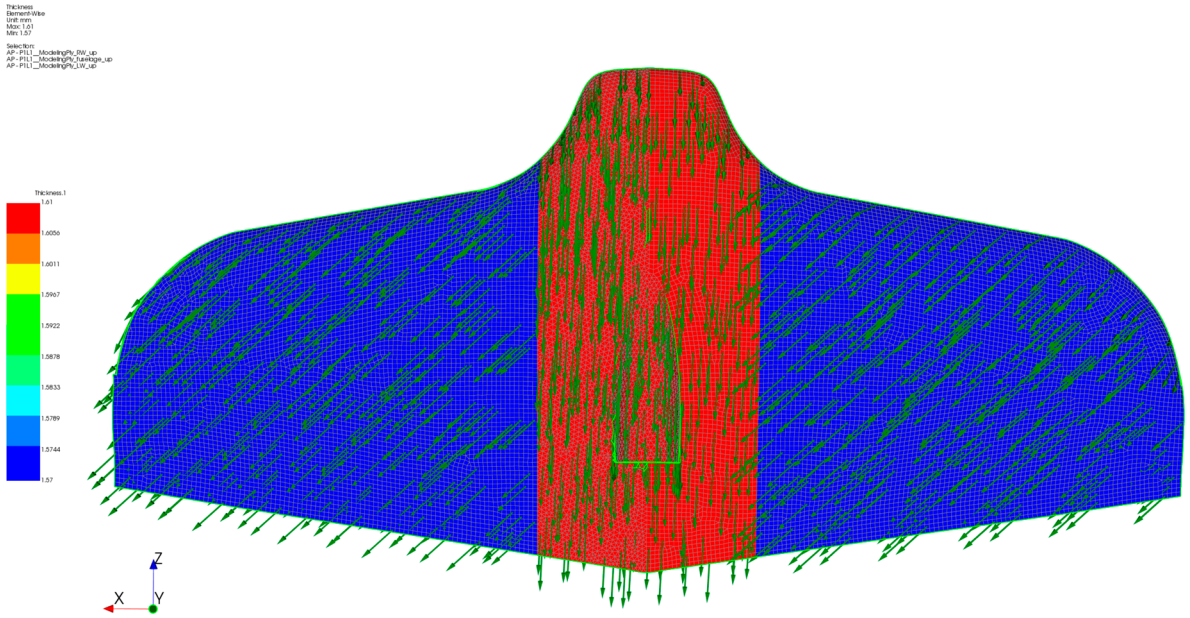

Figure 3. Direction of the plies assigned. Green arrows shows direction of ply.

Table 2. Material properties assigned in Ansys.

Property	CBX90	Torayca	Interglass
E_x, E_y [MPa]	38,093	50,952	10,000
G_{xy} [MPa]	3130	4883	2800
Density [g/cm^3]	1.51	1.62	1.27
Thickness [mm]	0.10	0.12	0.07

The modal analysis was conducted under free–free boundary conditions to replicate the unconstrained state of the structure during flight. This approach avoids the introduction of artificial stiffness that could distort the dynamic response. To prevent numerical issues associated with rigid body modes, the lower frequency threshold of the solver was set to 1 Hz.

2.3. Experimental Campaign

Experimental modal testing was performed on an aircraft suspended using a flexible support system to approximate free-flight boundary conditions (Figure 4).

The structure was supported at four suspension points using elastic cords, each characterized by an estimated stiffness of approximately 100 N/m. Assuming a parallel configuration of the suspension system, the equivalent stiffness is approximately 400 N/m. For the tested aircraft with an approximate mass of 3 kg, the resulting rigid-body natural frequency of the suspension system is about 2 Hz. Excitation was introduced with an electrodynamic shaker DEWESoft DS-MS-440, 440 N, 0–5 kHz (manufactured in Trbovlje, Slovenia).

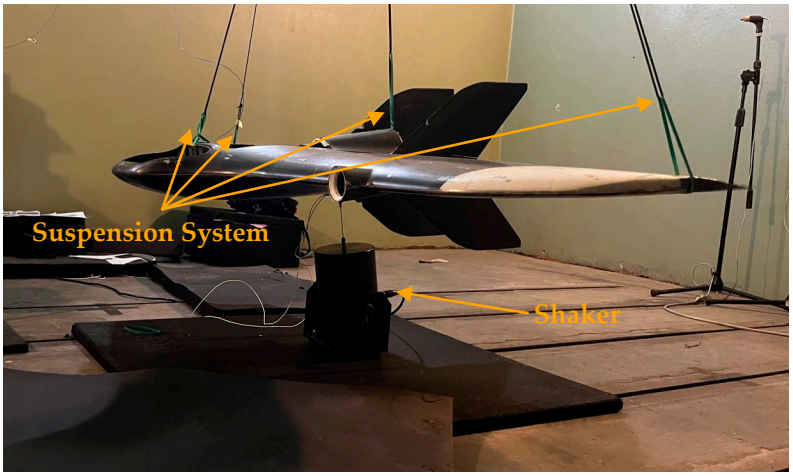

Figure 4. Experimental testing.

This approach ensured controlled and repeatable input signals (excitation point and signal is constants) while reducing the risk of structural damage that can occur when using an impact hammer. The excitation input was monitored and controlled using a Dytran 5860B IEPE impedance head (manufactured in Chatsworth, CA, USA), which integrates both a force transducer (100 mV/lbf) and an accelerometer (100 mV/g) within a single unit. The acceleration signal from the impedance head served as the feedback parameter in a closed-loop control system for the shaker amplifier. The structural response was captured using a lightweight, miniature triaxial piezoelectric IEPE accelerometer (PCB Piezotronics 356A03, 10 mV/g sensitivity, manufactured in Depew, NY, USA). The structure was excited using a sine sweep in the frequency range of 0–220 Hz. A two-stage sweep strategy was applied to ensure uniform energy distribution across the investigated frequency band. In the low-frequency range (0–40 Hz), a constant excitation level of 0.1 g was applied with a sweep rate of 1 Hz/s. In the higher frequency range (40–220 Hz), the excitation amplitude was gradually increased from 0.1 g to 2 g with a sweep rate of 5 Hz/s, in order to maintain sufficient signal-to-noise ratio while preserving linear system behavior.

Data acquisition was performed with an analog channel sampling rate of 10 kHz. The frequency resolution was set to 0.5 Hz, corresponding to 10,000 spectral lines. This configuration ensured adequate spectral resolution for accurate identification of modal parameters within the investigated frequency range.

The excitation location should be chosen to provide strong mechanical coupling between the structure and the exciter, allowing efficient transmission of vibrational energy. It is also essential to firmly mount the equipment at this point to eliminate any local looseness, as such imperfections may introduce nonlinear effects or cause unwanted resonances in the mounting system, ultimately compromising measurement accuracy.

During the selection of the excitation point, preliminary verification tests were conducted by measuring responses at critical locations. This ensured that the input energy was properly transmitted throughout the structure and that the chosen point was suitable.

A total of 94 measurement points were distributed across the upper surface to accurately represent the structural layout. The measurement grid was defined with consideration of the expected dominant deformation patterns of aircraft wing structures, in particular bending and torsional modes. For this reason, sensors were placed along both the leading and trailing edges as well as near the wing tip regions, where the largest modal displacements were anticipated. Additionally, local geometric constraints of the structure, including access limitations and cut-outs, required exclusion of several regions from measurement.

As a result, the final set of 94 measurement points was obtained as a practical compromise between spatial resolution, structural accessibility, and experimental feasibility.

The elevons were excluded from the measurements following recommendations from studies such as the NASA X-56A aircraft research [34]. The elevons were secured at a neutral (0-degree) position to minimize issues like drooping and measurement inconsistencies, thereby improving the reliability and repeatability of the test conditions.

Representative FRFs and coherence functions measured at selected response locations are shown in Figures 5 and 6 below. The observed responses confirm that the excitation energy is effectively transmitted across the entire structure. These results validate the selected excitation location, excitation signal parameters, and measurement point distribution adopted for the experimental modal analysis.

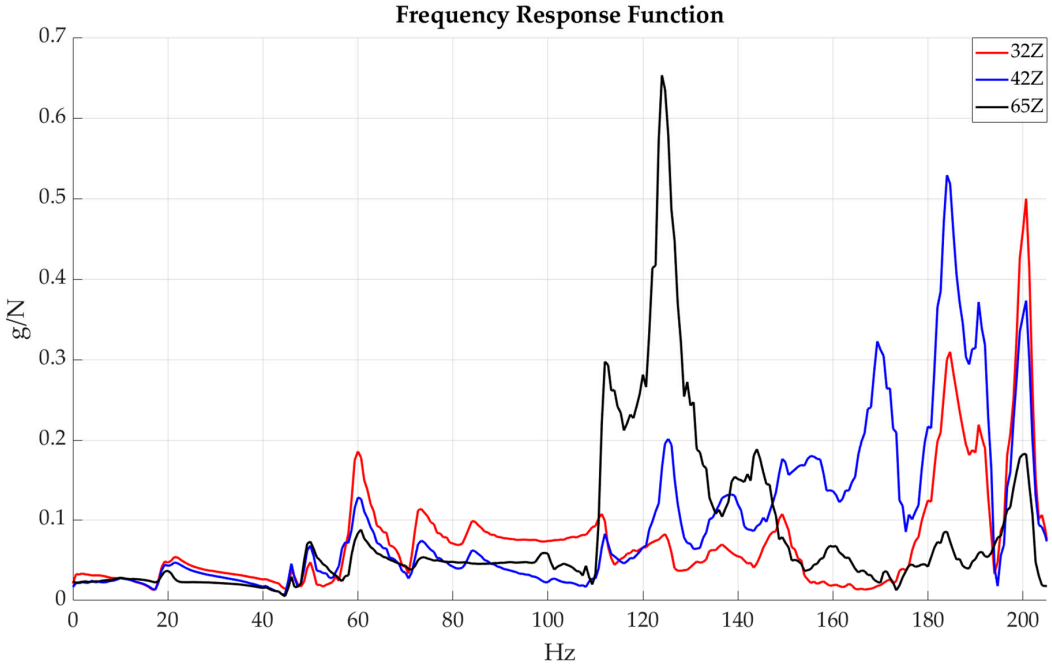

Figure 5. FRF for 3 measured points.

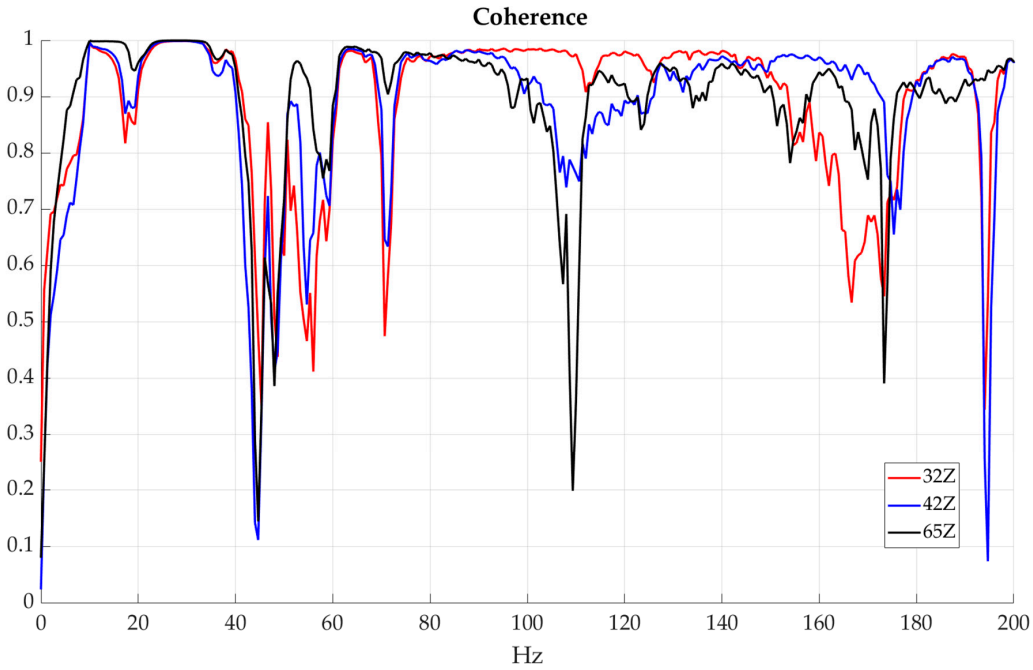

Figure 6. Coherence for 3 measured points.

3. Results

The Complex Mode Indication Function (CMIF) obtained from the experimental measurements is shown in Figure 7, with the identified natural frequencies indicated. The CMIF is a modal parameter estimation tool based on the singular value decomposition of the FRF matrix. It facilitates the identification of natural frequencies by highlighting resonant peaks associated with the structural modes while reducing the influence of measurement noise and closely spaced modes.

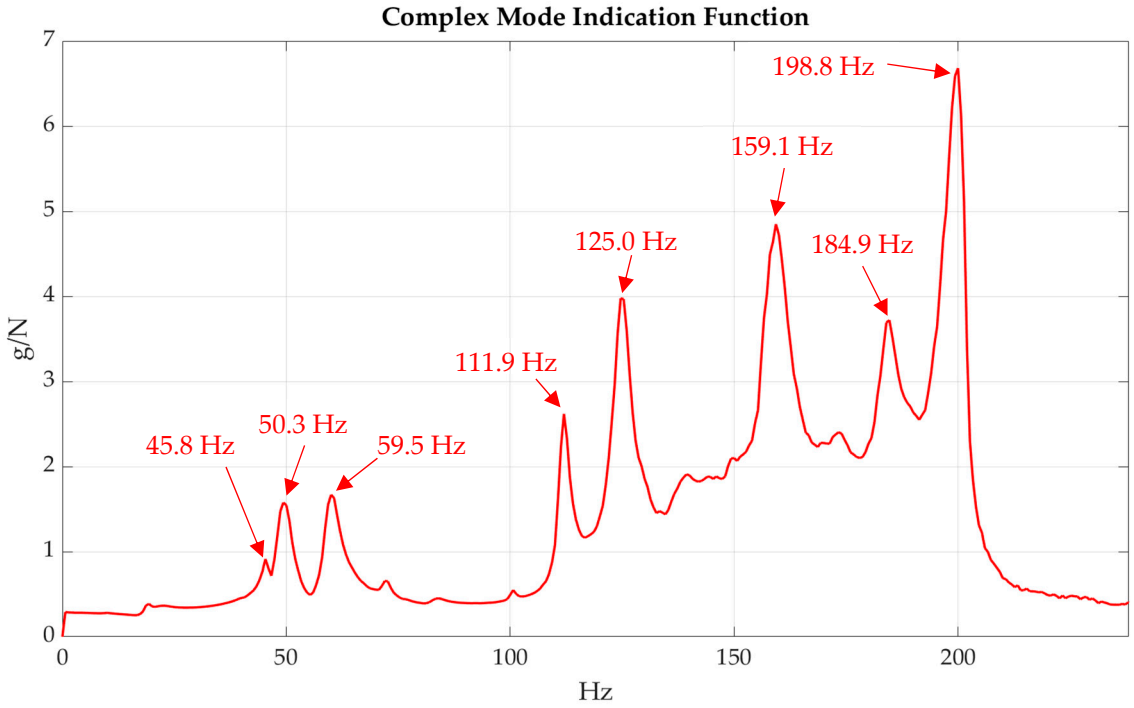

Figure 7. CMIF obtained from experimental testing.

From an aeroelastic perspective, the most important modes are the bending and torsional modes of the wing, as their interaction can lead to dynamic instabilities such as flutter. Therefore, particular attention was given to identifying and characterizing these modes during the modal analysis process. The experimentally and numerically identified bending and torsional modes are compared in Table 3.

Table 3. Comparison of experimental and numerical results.

Mode Type	Experiment [Hz]	Simulation [Hz]	Difference [%]
1st bending	50.3	60.4	20.08
2nd bending	111.9	97.8	12.6
1st torsional	125.0	138.0	10.4

The comparison of the mode shapes is presented in Figure 8 below.

Generally good agreement is observed for all identified modes, particularly in terms of mode shape correlation, which confirms that the numerical model captures the global dynamic behavior of the structure. Nevertheless, noticeable discrepancies in natural frequencies are present, reaching up to approximately 20% for the first bending mode.

Such differences are typical for lightweight composite structures and can be attributed to several modeling and experimental factors. First, the finite element model exhibits a tendency to overestimate structural stiffness, which is a common issue in simplified composite modeling approaches. In particular, the numerical representation assumes a

continuous and idealized structural layout, whereas the real structure contains cut-outs, local discontinuities, and manufacturing imperfections such as resin-rich areas resulting from the hand lay-up process, which locally alter stiffness and mass distribution. Moreover, the actual structure is not perfectly symmetric due to manufacturing tolerances, which further contributes to deviations between the numerical and experimental results. This leads to an overall stiffening of the numerical model and, consequently, higher predicted natural frequencies for selected modes.

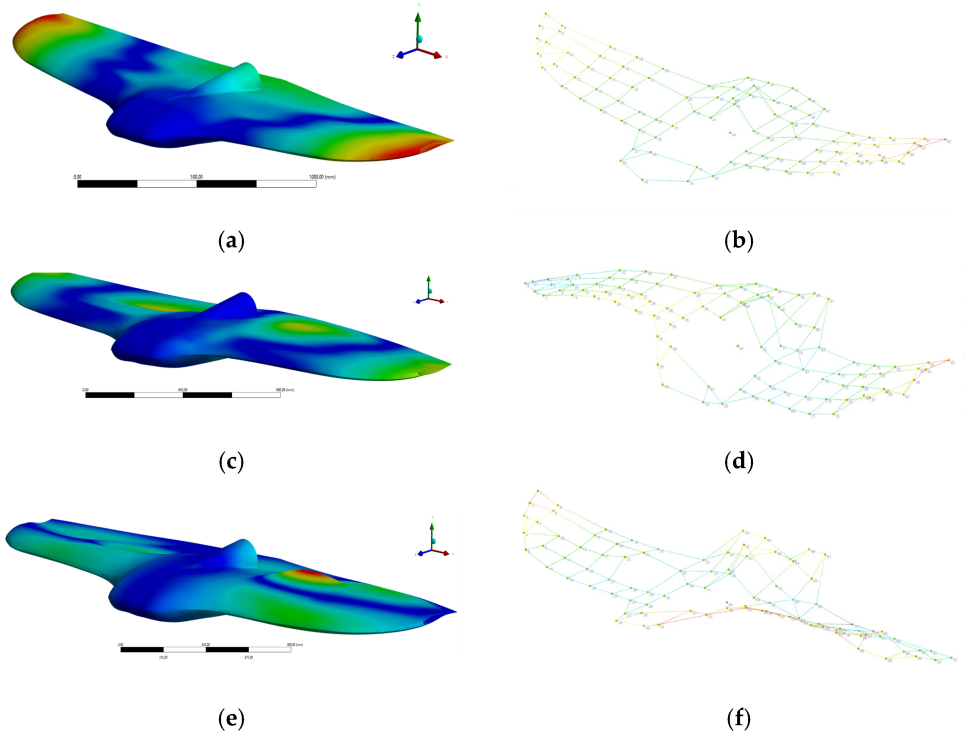

Figure 8. Mode shapes comparison: (**a**) 1st bending—simulation; (**b**) 1st bending—experiment; (**c**) 2nd bending—simulation; (**d**) 2nd bending—experiment; (**e**) 1st torsional—simulation; (**f**) 1st torsional—experiment.

Secondly, the mass distribution differs between the experimental and numerical configurations. In the physical test, the fins were mounted on the structure during measurements, introducing additional concentrated mass. This configuration was not fully reflected in the numerical model, which further contributes to deviations in both bending and torsional modes.

Additionally, the experimental procedure relied on a single accelerometer setup, requiring sequential measurements across multiple points. As a result, the structure was subjected to approximately 90 excitation cycles during the test campaign. Although no significant damage was observed, such repeated loading may have introduced minor changes in boundary conditions or local stiffness, which could have slightly influenced the final measured response.

In addition, a mesh convergence study was performed to ensure the numerical stability and independence of the results with respect to the finite element discretization. The results of this analysis, including the corresponding mesh sizes, predicted frequencies, and computational time, are summarized in Table 4. The study was carried out for the shell-based part of the model, which represents the most computationally demanding region due to its large spatial extent and higher element count.

Table 4. Mesh convergence study.

Shell Mesh Size [mm]	8	6	4
1st frequency [Hz]	60.4	60.3	60.1
2nd frequency [Hz]	97.8	97.3	97.0
3rd frequency [Hz]	138.0	137.5	137.1
Computational time [s]	55	109	204

It can be observed that further mesh refinement has a negligible influence on the identified natural frequencies, with variations below approximately 0.5% across all investigated modes. In contrast, the computational cost increases significantly with mesh refinement.

4. Conclusions

This study presented an experimental and numerical investigation of the dynamic behavior of a full-scale composite flying wing UAV. Ground vibration testing was performed to identify modal properties of the structure, with particular emphasis on bending and torsional modes relevant for future aeroelastic analyses and flutter prediction.

A finite element model of the structure was developed and validated against experimental results. Overall, a good agreement in mode shapes was achieved, confirming that the numerical model correctly captures the global dynamic behavior of the flying wing configuration. However, noticeable differences in natural frequencies were observed, reaching up to approximately 20%, particularly for the first bending mode.

It should be emphasized that the investigated configuration represents a full-scale, hand lay-up composite flying wing structure, which inherently introduces additional uncertainty compared to idealized or laboratory-scale structures. Manufacturing-induced imperfections, such as resin-rich regions, local stiffness variations, and geometric asymmetries, as well as structural discontinuities including cut-outs and assembly-related deviations, are difficult to fully capture in numerical modeling and contribute to the observed discrepancies. In addition, during the experimental GVT campaign, the fins were installed on the structure, which introduced additional concentrated mass and altered the overall mass distribution compared to the numerical model, further influencing both bending and torsional natural frequencies.

Despite these limitations, the obtained level of correlation is considered sufficient for preliminary aeroelastic assessment and provides a reliable basis for further dynamic investigations. In particular, the validated modal basis ensures that the most critical global deformation mechanisms, namely the dominant bending and torsional modes, are accurately represented in the numerical model.

The study also confirmed that mesh refinement beyond the selected discretization level has negligible influence on the predicted modal parameters, while significantly increasing computational cost. This supports the robustness of the adopted modeling approach and confirms the adequacy of the selected finite element mesh for modal analysis purposes.

From a methodological perspective, the results highlight the importance of combining experimental modal testing with numerical model updating in lightweight composite airframe structures, where simplified modeling assumptions can lead to stiffness overestimation. The presented workflow demonstrates a practical approach for correlating experimental GVT data with finite element predictions under realistic engineering constraints.

For future work, the model can be further improved by incorporating more detailed representations of local structural features, refined mass distribution modeling, and advanced experimental techniques such as multi-sensor or non-contact measurements to eliminate potential measurement bias. Additionally, the validated model provides a solid

foundation for subsequent aeroelastic analyses, including flutter prediction and dynamic stability assessment under coupled aerodynamic loading conditions.

Overall, the presented results contribute to the understanding of dynamic behavior in ultralight composite flying wing UAV configurations and demonstrate the applicability of combined experimental–numerical approaches for structural dynamics characterization in complex aerospace systems.

Author Contributions: Conceptualization, M.M., M.K. and K.K.; methodology, M.M., B.D. and J.N.; software, K.K., B.D. and J.N.; validation, M.M., J.W. and P.B.; formal analysis, M.M., M.K. and P.B.; investigation, M.M., J.W. and P.B.; resources, M.K., B.D., K.K. and J.N.; data curation, M.M., J.W., M.K. and J.N.; writing—original draft preparation, M.M., M.K., K.K., B.D. and J.N.; writing—review and editing, J.W., P.B., T.K. and A.K.; visualization, J.W. and P.B.; supervision, J.W., T.K. and A.K.; project administration, T.K. and A.K.; funding acquisition, T.K. and A.K. All authors have read and agreed to the published version of the manuscript.

Funding: This research was funded by the National Centre for Research and Development, under the LIDER XIV programme, grant no. 0292/L-14/2023, project "Bezzałogowy płatowiec szybkiego reagowania dostarczający defibrylator osobom z NZK".

Institutional Review Board Statement: Not applicable.

Informed Consent Statement: Not applicable.

Data Availability Statement: The raw data supporting the conclusions of this article will be made available by the authors on request.

Conflicts of Interest: The authors declare no conflicts of interest.

References

1. Butilă, E.V.; Boboc, R.G. Urban Traffic Monitoring and Analysis Using Unmanned Aerial Vehicles (UAVs): A Systematic Literature Review. *Remote Sens.* **2022**, *14*, 620. [CrossRef]
2. Aurambout, J.-P.; Gkoumas, K.; Ciuffo, B. Last Mile Delivery by Drones: An Estimation of Viable Market Potential and Access to Citizens across European Cities. *Eur. Transp. Res. Rev.* **2019**, *11*, 30. [CrossRef]
3. Mohamed, A.; Mohamed, M. Unmanned Aerial Vehicles in Last-Mile Parcel Delivery: A State-of-the-Art Review. *Drones* **2025**, *9*, 413. [CrossRef]
4. Aliane, N. Drones and AI-Driven Solutions for Wildlife Monitoring. *Drones* **2025**, *9*, 455. [CrossRef]
5. Chand, B.; Ayele, F.; Pineiro-Dakers, I.; Samsami, R.; Chang, B. Uncrewed Aerial System (UAS) Applications in Bridge Inspection: A Comprehensive Review of Platforms, Sensors, and Operational Effectiveness. *Drones* **2026**, *10*, 144. [CrossRef]
6. Barmpounakis, M.; Espadaler-Clapés, J.; Tsitsokas, D.; Mordan, T.; Geroliminis, N. A New Perspective on Urban Mobility Through Large-Scale Drone Experiments for Smarter, Sustainable Cities. *Drones* **2025**, *9*, 637. [CrossRef]
7. Traub, L.W. Wing Efficiency Enhancement at Low Reynolds Number. *Aerospace* **2024**, *11*, 320. [CrossRef]
8. Matos, N.M.B.; Marta, A.C. Aerodynamic Shape Optimization of Wing–Fuselage Intersection for Minimum Interference Drag. *Aerospace* **2025**, *12*, 369. [CrossRef]
9. Nikolaou, E.; Kilimtzidis, S.; Kostopoulos, V. Winglet Design for Aerodynamic and Performance Optimization of UAVs via Surrogate Modeling. *Aerospace* **2025**, *12*, 36. [CrossRef]
10. Karpenko, M.; Stosiak, M.; Deptuła, A.; Urbanowicz, K.; Nugaras, J.; Królczyk, G.; Żak, K. Performance Evaluation of Extruded Polystyrene Foam for Aerospace Engineering Applications Using Frequency Analyses. *Int. J. Adv. Manuf. Technol.* **2023**, *126*, 5515–5526. [CrossRef]
11. Poojary, U.R.; Hegde, S. Experimental Investigation of Influence of Fibre Orientation on the Dynamic Properties of Carbon Fibre and Intra-Ply Woven Carbon-Kevlar/Epoxy Hybrid Composite. *J. Compos. Sci.* **2024**, *8*, 78. [CrossRef]
12. Jones, R.M. *Mechanics Of Composite Materials*, 2nd ed.; CRC Press: Boca Raton, FL, USA, 2018.
13. Franz, M.; Radjef, R.; Eisenbart, B.; Wartzack, S. Effects of Ply Misalignment in Material Characterization of Composite Laminates. *Fibers* **2024**, *12*, 103. [CrossRef]
14. Gupta, A.; Seiler, P.J.; Danowsky, B.P. Ground Vibration Tests on a Flexible Flying Wing Aircraft—Invited. In *AIAA Atmospheric Flight Mechanics Conference*; AIAA SciTech Forum; American Institute of Aeronautics and Astronautics: Reston, VA, USA, 2016.
15. Dessena, G.; Ignatyev, D.I.; Whidborne, J.F.; Pontillo, A.; Zanotti Fragonara, L. Ground Vibration Testing of a Flexible Wing: A Benchmark and Case Study. *Aerospace* **2022**, *9*, 438. [CrossRef]

16. Dinulović, M.; Perić, M.; Stamenković, D.; Bengin, A.; Adžić, V.; Trninić, M. Aeroelastic Behavior of 3D-Printed Tapered Polylactic Acid Plates Under Subsonic Flow Conditions. *Materials* **2025**, *18*, 1127. [CrossRef] [PubMed]
17. Leone, D.D.; Balbo, F.L.; Gaspari, A.D.; Ricci, S. Model Updating and Aeroelastic Correlation of a Scaled Wind Tunnel Model for Active Flutter Suppression Test. *Aerospace* **2021**, *8*, 334. [CrossRef]
18. Friswell, M.I.; Mottershead, J.E. *Finite Element Model Updating in Structural Dynamics*; Solid Mechanics and its Applications; Springer: Dordrecht, The Netherlands, 1995; Volume 38.
19. Guo, L.; Liu, J.; Song, B.; Pan, G.; Liu, Y. Vibration Analysis and Suppression Methods of the Wing of an Underwater Glider. *Int. J. Acoust. Vib.* **2023**, *28*, 249–257. [CrossRef]
20. Simsiriwong, J.; Sullivan, R.W. Experimental Vibration Analysis of a Composite UAV Wing. *Mech. Adv. Mater. Struct.* **2012**, *19*, 196–206. [CrossRef]
21. Guan, Y.; Xu, W.; Zhang, M. Nonlinear Modeling of Composite Wing with Application to UAV Flight Dynamic Analysis. *Mech. Syst. Signal Process.* **2020**, *138*, 106542. [CrossRef]
22. Georgiou, G.; Manan, A.; Cooper, J.E. Modeling Composite Wing Aeroelastic Behavior with Uncertain Damage Severity and Material Properties. *Mech. Syst. Signal Process.* **2012**, *32*, 32–43. [CrossRef]
23. Ruseno, N. Modal Analysis Of Blended Wing-Body UAV. *J. Teknol. Kedirgant.* **2021**, *6*, 68–75. [CrossRef]
24. Chakravarty, U.K. Modal Analysis of a Composite Wing of Micro Air Vehicle. *J. Aircr.* **2011**, *48*, 2175–2178. [CrossRef]
25. Pavan Kishore, M.L.; Madhavi, B.; Pati, P.R.; Pugazhenthi, R.; Giri, J.; Sathish, T.; Parthiban, A. Free Vibration Analysis of Composite Aircraft Wing. *Interactions* **2024**, *245*, 125. [CrossRef]
26. Tandel, K.S.; Thanujj, P.S.; Rachana, P.M.; Nagaraju, K.P.; Bhanumurthy, R.; Prajwal, T.R. Fluid-Structure Interaction Analysis of High Aspect Ratio Composite Wing Structures. In *Proceedings of the 2024 IEEE International Conference on Electronics, Computing and Communication Technologies (CONECCT)*; IEEE: New York, NY, USA, 2024; pp. 1–6.
27. Ji, Z.; Guo, T.; Zhou, D.; Lu, Z.; Lyu, B. Time-Domain Analysis of Body Freedom Flutter Based on 6DOF Equation. *CMES* **2023**, *138*, 489–508. [CrossRef]
28. Guo, S.; Jing, Z.W.; Li, H.; Lei, W.T.; He, Y.Y. Gust Response and Body Freedom Flutter of a Flying-Wing Aircraft with a Passive Gust Alleviation Device. *Aerosp. Sci. Technol.* **2017**, *70*, 277–285. [CrossRef]
29. Qaumi, T.; Hashemi, S.M. Experimental and Numerical Modal Analysis of a Composite Rocket Structure. *Aerospace* **2023**, *10*, 867. [CrossRef]
30. Chadha, A.; Sudhagar, P.E.; Subramani, M. Numerical and Experimental Investigation on Vibration Analysis of Laminated Composite Conical Shell Structures. *AIP Conf. Proc.* **2021**, *2341*, 020013. [CrossRef]
31. *ASTM D3039*; Standard Test Method for Tensile Properties of Polymer Matrix Composite Maerials. ASTM International: West Conshohocken, PA, USA, 2025.
32. *ASTM D6641*; Standard Test Method for Compressive Properties of Polymer Matrix Composite Materials Using a Combined Loading Compression (CLC) Test Fixture. ASTM International: West Conshohocken, PA, USA, 2021.
33. *ASTM D7078*; Standard Test Method for Shear Properties of Composite Materials by V-Notched Rail Shear Method. ASTM International: West Conshohocken, PA, USA, 2025.
34. Chin, A.W.; Truong, S.; Spivey, N. X-56A Structural Dynamics Ground Testing Overview and Lessons Learned. In Proceedings of the AIAA Scitech 2020 Forum; American Institute of Aeronautics and Astronautics: Orlando, FL, USA, 2020.